Supporting Information

Defluorination of Per- and Polyfluoroalkyl Substances (PFASs) with Hydrated Electrons: Structural Dependence and Implications to PFAS Remediation and Management

Michael J. Bentel,[†] Yaochun Yu,[‡] Lihua Xu,[†] Zhong Li,[∥] Bryan M. Wong,[†,§] Yujie Men,[‡,⊥] and Jinyong Liu[*,†]

[†]Department of Chemical & Environmental Engineering and [§]Materials Science & Engineering Program, University of California, Riverside, California, 92521, United States

[‡]Department of Civil & Environmental Engineering, [∥]Metabolomics Lab of Roy J. Carver Biotechnology Center, and [⊥]Institute for Genomic Biology, University of Illinois at Urbana–Champaign, Urbana, Illinois, 61801, United States

Corresponding Author

*(J.L.) E-mail: jyliu@engr.ucr.edu; jinyong.liu101@gmail.com.

Table of Contents

Detailed Information on Materials and Methods

Chemicals and the Preparation of PFAS Stock Solutions. All PFAS chemicals were purchased from Acros Organics, Alfa-Aesar, MP Biomedicals, Oakwood Chemicals, Sigma-Aldrich, and SynQuest Laboratories. **Table A1** (next page) summarizes the name, purity, and CAS number of all PFASs included in this study. All other chemicals and solvents were purchased from Fisher Chemical. Individual PFASs were dissolved in either deionized (DI, produced by Milli-Q system) water as 10 mM stock solutions. For carboxylic acids, the addition of 20 mM NaOH (for PFCAs) or 40 mM NaOH (for PFdiCAs) effectively facilitated the dissolution of long chain structures in water and prevented the volatilization of short chain structures. For long chain FTCAs (more than 8 carbons in the molecule), methanol was used as the solvent. Methanol does not interfere with the PFAS defluorination with hydrated electrons. For example, preliminary experiments with 25 μM PFOA introduced with the water stock solution (1.5 mL into 600 mL final volume) and with the methanol stock solution (0.3 mL into 600 mL final volume, resulting in ~12 mM methanol in water) gave the same rate and extent of defluorination. All PFAS stock solutions were stored at 4°C.

Table A1. Information of PFASs Used in This Study.

Entry	Chemical Name	Fluoroalkyl	Length (n)	Purity	CAS#
		$F(CF_2)_n$–COOH (or salt)			
1	Sodium trifluoroacetate		1	98%	2923-18-4
2	Perfluoropropionic acid		2	97%	422-64-0
3	Perfluorobutyric acid		3	98%	375-22-4
4	Perfluoropentanoic acid		4	97%	2706-90-3
5	Perfluorohexanoic acid		5	97%	307-24-4
6	Perfluoroheptanoic acid		6	98%	375-85-9
7	Perfluorooctanoic acid		7	96%	335-67-1
8	Perfluorononanoic acid		8	97%	375-95-1
9	Perfluorodecanoic acid		9	97%	335-76-2
10	Perfluoroundecanoic acid		10	96%	2058-94-8
		HOOC–$(CF_2)_n$–COOH			
11	Difluoromalonic acid		1	98%	1514-85-8
12	Tetrafluorosuccinic acid		2	98%	377-38-8
13	Hexafluoroglutaric acid		3	98%	376-73-8
14	Octafluoroadipic acid		4	97%	336-08-3
15	Dodecafluorosuberic acid		6	98%	678-45-5
16	Tetradecafluoroazelaic acid		7	90%	23453-64-7
17	Hexdecafluorosebacic acid		8	95%	307-78-8
18	Perfluoro-1,10-decanedicarboxylic acid		10	96%	865-85-0
		$F(CF_2)_n$–CH_2CH_2–COOH			
19	4,4,4-Trifluorobutyric acid		1	99%	406-93-9
20	2H,2H,3H,3H-Perfluoropentanoic acid		2	N/A	3637-31-8
21	2H,2H,3H,3H-Perfluorohexanoic acid		3	97%	356-02-5
22	2H,2H,3H,3H-Perfluoroheptanoic acid		4	97%	80705-13-1
23	2H,2H,3H,3H-Perfluorooctanoic acid		5	N/A	914637-49-3
24	2H,2H,3H,3H-Perfluorononanoic acid		6	97%	27854-30-4
25	2H,2H,3H,3H-Perfluorodecanoic acid		7	97%	812-70-4
26	2H,2H,3H,3H-Perfluoroundecanoic acid		8	97%	34598-33-9
		$F(CF_2)_n$–SO_3H (or salt)			
27	Sodium trifluoromethanesulfonate		1	98%	2926-30-9
28	Potassium nonafluorobutanesulfonate		4	98%	29420-49-3
29	Potassium perfluorohexane-1-sulfonate		6	95%	3871-99-6
30	Perfluorooctanesulfonic acid		8	97%	1763-23-1
		Special structures			
31	2,2-difluorosuccinic acid	**HOOC–CF_2CH_2–COOH**		97%	665-31-6
32	3,3,3-Trifluoropropionic acid	**CF_3–CH_2–COOH**		97%	2516-99-6
33	Difluoroacetic acid	**CF_2H–COOH**		98%	381-73-7
34	Sodium fluoroacetate	**CFH_2–COONa**		98%	62-74-8

Defluorination Reaction Settings. A 600-mL solution containing 25 μM PFAS, 10 mM Na_2SO_3, and 5 mM $NaHCO_3$ (pH 9.5, adjusted by 0.5 mL of 1 M NaOH) was prepared with DI water. Powders of Na_2SO_3 (756 mg) and $NaHCO_3$ (252 mg) were used to prepare each fresh solution without on-shelf storage in solution. The closed-system cylindrical photochemical reactor consisted of a borosilicate glass shell and a quartz immersion well, both of which are double-layered for cooling with circulated water (20°C) in the jacket. The space between the glass shell and immersion well (~2 cm thickness ring column) was loaded with the 600-mL reaction solution. A magnetic stir bar was placed at the bottom of the reactor, and the stirring speed was set at 360 rpm. An 18 W low-pressure mercury lamp (GPH212T5L/4P/HO, "High Output") in the immersion well delivered 254 nm UV irradiation to the surrounding solution. A previous report[1] has described the photochemical parameters of a system with the same key dimension of both the photoreactor and the UV lamp (except that the power of GPH212T5L/4P lamp in that report was 10 W). The reactor assembly was wrapped in heavy-duty aluminum foil to prevent UV irradiation leaking. After the UV lamp was turned on, aliquots of solution (5 mL each) were taken at time intervals through a 16-gauge stainless steel needle that penetrated the rubber-sealed sampling port. The samples were stored in 7-mL glass scintillation vials at 4°C prior to analysis.

Two reasons for choosing sulfite as the e_{aq}^- source are (1) the resulting sulfate is a ubiquitous natural water mineral, and (2) sulfite can be economically obtained from coal combustion flue gas scrubbing.[2] The reason for choosing carbonate as the buffer/additive is that carbonate is ubiquitous in all natural waters, especially in groundwater. Reaction conditions tested in this study and reported in the literature on PFOA/PFOS defluorination are summarized in **Table A2** (next page). During the preliminary tests, the N_2 sparging step prior to the photochemical reaction did not show significant enhancement to the defluorination from PFOA (e.g., **entry 1** vs. **2**, and **entry 3** vs. **4** although other parameters were slightly different) probably because the added 10 mM Na_2SO_3 far exceeded the dissolved oxygen (the saturated DO level at 20°C is 9.0 mg L^{-1} or 0.28 mM). Thus, most reactions in this study did not have the N_2 sparging step for DO removal. During the preliminary tests, the $NaHCO_3$ buffer and NH_4Cl buffer at pH 9.2−9.5 showed no significant influence on the defluorination of PFOA (e.g., **entry 3** vs. **7**). When 10 mM Na_2SO_3 was used, the maximum defluorination ratio of PFOA and PFOS were also similar to (or even slightly higher than) the previous reports that used a high-pressure UV lamp (250 W, high photon flux with a wide irradiation spectrum of 200–600 nm),[3, 4] Na_2SO_3 or potassium iodide (KI) as the electron source chemical,[5, 6] or nitrilotriacetic acid (NTA) as the hydroxyl radical scavenger.[7] Thus, the experimental setting of this study can be representative for the reported systems using variable hydrated electron source chemicals and UV lamps.

Table A2. Summary of Experimental Conditions for PFOA/PFOS Defluorination.

Entry	Reaction Condition	Buffer Chemical[a]	pH	N_2 Sparge	Reaction Time	DeF Ratio	Reference
		PFOA defluorination reactions					
1	25 μM PFOA; 254 nm (18W); 10 mM Na_2SO_3; 20°C	$NaHCO_3$ (5mM)	9.5	1 h	12 h	49%	This study
2	25 μM PFOA; 254 nm (18W); 10 mM Na_2SO_3; 20°C	$NaHCO_3$ (5mM)	9.5	No sparge	12 h	48%	This study
3	25 μM PFOA; 254 nm (18W); 10 mM Na_2SO_3; 20°C	$NaHCO_3$ (5mM)	9.5	No sparge	48 h	57%	This study
4	20 μM PFOA; 254 nm (10W); 10 mM Na_2SO_3; 25°C	NH_4OH	9.3	30 min	24 h	63%	[6]
5	39 μM PFOA; 200− 400 nm (<250 W);[b] 10 mM Na_2SO_3; 25°C	Not added	9.2	No sparge	10 min	46%	[4]
6	25 μM PFOA; 254 nm (18 W); 0.3 mM KI; 20°C	NH_4Cl (5 mM)	9.3	1 h	8 h	34%	This study
7	25 μM PFOA; 254 nm (18 W); 1.0 mM KI; 20°C	NH_4Cl (5 mM)	9.3	1 h	22 h	58%	This study
8	25 μM PFOA; 254 nm (15 W); 0.3 mM KI; room temperature	NH_4Cl	9.0	30 min	14 h	99%[c]	[5]
9	25 μM PFOA; 254 nm (15 W); 0.3 mM KI; room temperature	NH_4Cl	9.0	30 min	8 h	85%[c]	[5]
		PFOS defluorination reactions					
10	25 μM PFOS; 254 nm (18W); 10 mM Na_2SO_3; 20°C	$NaHCO_3$ (5mM)	9.5	No sparge	48 h	56%	This study
11	25 μM PFOS; 254 nm (18W); 10 mM Na_2SO_3; 20°C	$NaHCO_3$ (5mM)	9.5	No sparge	12 h	38%	This study
12	32 μM PFOS; 200− 400 nm (<250 W);[b] 10 mM Na_2SO_3; 25°C	Not added	9.2	No sparge	30 min	56%	[3]
13	10 μM PFOS; 254 nm (14W); 2 mM NTA; 30°C	NH_4Cl	10.0	20 min	10 h	47%	[7]
14	10 μM PFOS; 254 nm (14W); 2 mM Na_2SO_3; 30°C	NH_4Cl	10.0	20 min	10 h	30%	[7]

[a]NaOH and NH_4OH were used to raise the pH of solutions added with $NaHCO_3$ and NH_4Cl, respectively.
[b]The 400−600 nm portion was blocked so the effective irradiation power to the solution was reduced.
[c]Results are questionable because 99% and 85% defluorination of 0.025 mM PFOA ($C_7F_{15}COOH$) would require cleaving 0.37 mM and 0.32 mM C−F bonds, respectively. However, the KI concentration was only 0.30 mM. The maximum C−F cleavage, assuming 100% reaction efficiency of e_{aq}^- excited from KI, could be only 0.15 mM based on the theoretical 2:1 stoichiometry,[8] where both C and F need one electron after the bond cleavage.

Measurement of PFAS Parent Compound Decay. Concentrations of ionic PFAS parent compounds were analyzed by a high performance liquid chromatography–triple quadrupole mass spectrometry system (HPLC−MS/MS, Agilent 1200 HPLC, and Sciex 5500 QTRAP MS) in the Metabolomics Lab of Roy J. Carver Biotechnology Center at UIUC. The Analyst 1.6.2 software was used for data acquisition and analysis. For HPLC separation, a 10-μL sample was loaded onto a Zorbax SB-Aq column (particle size 5μm, 4.6×50 mm, Agilent) eluted with 350 μL min^{-1} of 10 mM ammonia formate (A) and methanol (B). The linear gradient was as follows: 100% A for 0−1 min, 2% A for 2−15 min, and 100% A for 16−21 min. The mass spectra were acquired under negative ionization (ESI) mode. The ion spray voltage was set to −4500 V, and the source temperature was set to 450 °C. The curtain gas, ion source gas 1, and ion source gas 2 flow were set to 30, 50, and 60 psi, respectively. Multiple reaction monitoring (MRM) was used for quantification, and the MRM transition was listed in **Table A3**. The limit of quantification (LOQ) for each compound was determined as the lowest concentration with a detection variation < 20%, which was listed in **Table A3**. An ion chromatography system (see below) was used for the quantification of short-chain PFASs ($CF_3CO_2^-$, $CF_2HCO_2^-$, $CFH_2CO_2^-$, and $CF_3SO_3^-$).

PFAS Transformation Product Analysis. PFAS transformation products were measured by liquid chromatography coupled with a high-resolution quadrupole orbitrap mass spectrometer (LC-HRMS/MS) (Q Exactive, Thermo Fisher Scientific). The LC analysis was the same as above described. The transformation products were detected in full scan negative ionization mode on HRMS at a resolution of 70,000 at m/z 200 and a scan range of m/z 50−750. The software Xcalibur (Thermo Fisher Scientific) was used for data acquisition and analysis.

Suspect screening was carried out to identify transformation products as previously described, but with slightly modification.[9, 10] Briefly, suspect screening was done by TraceFinder 4.1 EFS (Thermo Fisher Scientific). The transformation product suspect lists were generated by a self-written automatic product mass prediction script, which includes all possible products from the mechanisms of both chain shortening and H/F exchange. Plausible transformation products were identified based on the following criteria: (i) mass tolerance < 5 ppm; (ii) isotopic pattern score > 70%; (iii) peak area > 10^5; (iv) peak area showing increasing or first increase then followed by a decrease trend over time. The limit of quantification (LOQ) of known compounds are 100 nM for PFCAs and PFSAs, and 10 nM for FTCAs.

Quality Assurance and Quality Control (QA/QC). To take into account the matrix effect on the LC-MS/MS quantification of various PFASs investigated in this study, a PFAS-free solution from the photoreactor (i.e., all inorganic chemicals added and treated under the same UV irradiation) was used to prepare the calibration standards. The matrix-match standard series included nine points from 1 nM to 5 μM. MilliQ water and matrix blank controls were included, where no PFASs were detected on LC-MS/MS. MilliQ water blanks were also ran between each group of batch experiment samples and checked for PFASs detection in the blanks, to avoid PFAS carry over. The storage time for all samples was less than three weeks at 4°C.

Table A3. MRM Transition and LOQ.

Entry	Chemical Name	Chain Length (n)	MRM Transition (m/z)	LOQ(nM)
	$F(CF_2)_n$–COOH (or salt)			
1	Sodium trifluoroacetate	1	113.0/69.0	200
2	Perfluoropropionic acid	2	163.0/119.0	200
3	Perfluorobutyric acid	3	213.0/169.0	100
4	Perfluoropentanoic acid	4	263.0/219.0	25
5	Perfluorohexanoic acid	5	313.0/269.0	2
6	Perfluoroheptanoic acid	6	363.0/319.0	1
7	Perfluorooctanoic acid	7	413.0/369.0	2
8	Perfluorononanoic acid	8	463.0/419.0	1
9	Perfluorodecanoic acid	9	513.0/469.0	2
10	Perfluoroundecanoic acid	10	563.0/519.0	10
	HOOC–$(CF_2)_n$–COOH			
11	Difluoromalonic acid	1	139.0/95.0	200
12	Tetrafluorosuccinic acid	2	189.0/101.0	50
13	Hexafluoroglutaric acid	3	239.0/131.0	5
14	Octafluoroadipic acid	4	289.0/181.0	1
15	Dodecafluorosuberic acid	6	389.0/281.0	20
16	Tetradecafluoroazelaic acid	7	439.0/331.0	50
17	Hexdecafluorosebacic acid	8	489.0/381.0	50
18	Perfluoro-1,10-decanedicarboxylic acid	10	589.0/481.0	1
	$F(CF_2)_n$–CH_2CH_2–COOH			
19	4,4,4-Trifluorobutyric acid	1	141.0/121.0	50
20	2H,2H,3H,3H-Perfluoropentanoic acid	2	191.0/127.0	50
21	2H,2H,3H,3H-Perfluorohexanoic acid	3	241.0/177.0	50
22	2H,2H,3H,3H-Perfluoroheptanoic acid	4	291.0/167.0	20
23	2H,2H,3H,3H-Perfluorooctanoic acid	5	341.0 /237.0	5
24	2H,2H,3H,3H-Perfluorononanoic acid	6	391.0/287.0	5
25	2H,2H,3H,3H-Perfluorodecanoic acid	7	441.0/337.0	2
26	2H,2H,3H,3H-Perfluoroundecanoic acid	8	491.0/387.0	2
	$F(CF_2)_n$–SO_3H (or salt)			
27	Sodium trifluoromethanesulfonate	1	149.0/80.0	1
28	Potassium nonafluorobutanesulfonate	4	299.0/80.0	5
29	Potassium perfluorohexane-1-sulfonate	6	399.0/80.0	1
30	Perfluorooctanesulfonic acid	8	499.0/80.0	2
	Special structures			
31	2,2-difluorosuccinic acid **HOOC–CF_2CH_2–COOH**		153.0/89.0	50

Measurement of Fluoride Ion Release. The concentration of fluoride ion (F^-) released from PFASs was primarily determined by an ion selective electrode (ISE, Fisherbrand accumet solidstate) connected to a Thermo Scientific Orion Versa Star Pro meter. A 2-mL aliquot of reaction sample was added in the equal volume of the total ionic strength adjustment buffer (TISAB for fluoride electrode, Thermo Scientific), and the F^- concentration was determined with the ISE. The accuracy of F^- measurement by the ISE in the solution matrix was validated by the measurement of representative reaction samples using ion chromatography (**Figure A1**). A Dionex ICS-5000 ion chromatography system equipped with a conductivity detector and a Dionex IonPac AS11-HC column (4×250 mm) with a AG11-HC guard column (4×50 mm) was used for the ISE validation and the quantification of C2 short-chain PFASs. The samples were diluted for 10 fold with DI water. The column was used at 30°C, with a 20 mM NaOH isocratic eluent at 1.5 mL min^{-1}, and a suppressor current at 75 mA.

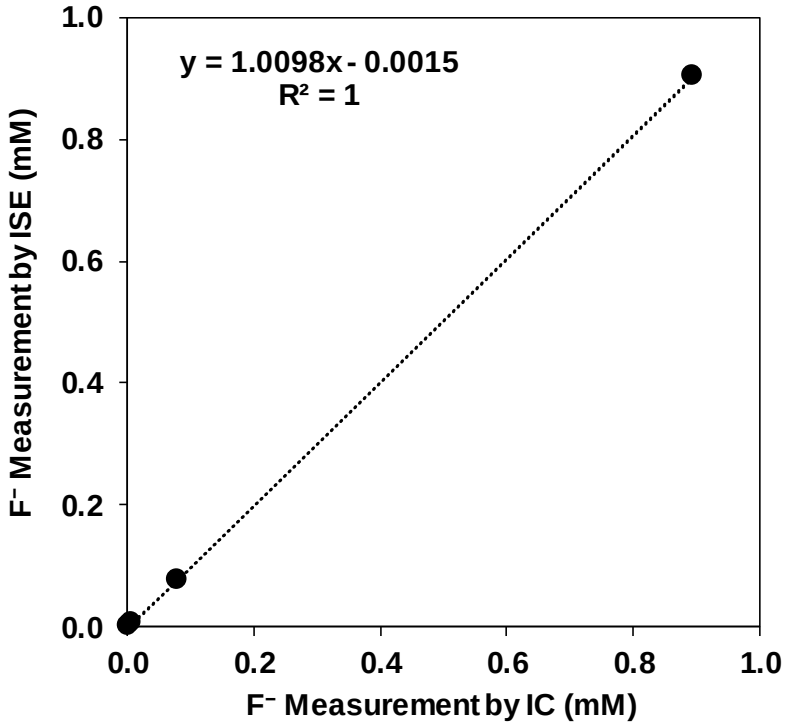

Figure A1. Fluoride measurement comparison between the ion chromatography (IC) and the fluoride ion-selective electrode (ISE) in samples with the reaction solution matrix.

DFT Calculation of C−F Bond Dissociation Energies (BDEs). The C−F BDEs for all PFASs examined in this study were calculated using the GAUSSIAN 09 software package.[11] All molecular geometries were fully optimized with the Grimme empirical dispersion correction with the Becke-Johnson damping term (D3-BJ)[12] added to the B3LYP/6-311+G(2d,2p) hybrid functional energies.[13-16] We have specifically chosen this level of theory to allow for a straightforward comparison with previous studies on similar compounds.[17] Truhlar's SMD solvation model was chosen to implicitly simulate the aqueous environment.[18] Harmonic frequency calculations were carried out to confirm that all of the structures were local minima on the potential energy surface. The BDE for each bond was calculated through the following expression:

$$E_{BDE} = \left(H^*_{radical[PFAS\ minus\ F]} + H^*_{radical\ F}\right) - H^*_{parent\ PFAS}$$

where H^* represents the enthalpy of formation.[17] Calculation results are summarized in **Tables S1−S5**.

Because a detailed defluorination mechanism remains elusive, in this study we still chose to calculate the energy for C−F bond dissociation to investigate a simplified correlation with the rate and extent of defluorination. We point out that since the reactions with e_{aq}^- will involve radical structures from the parent PFAS compounds and the release of fluoride ion, neither homolytic (i.e., forming a C radical and an F radical) nor heterolytic dissociation (i.e., forming a C cation and an F anion) of the ideal structures could reflect the exact reactions. However, the C−F BDEs can be used as a predictive descriptor because (1) the calculation results agree well with experimental findings, and (2) it provides a quick tool to predict the susceptibility to defluorination in an engineered treatment system using e_{aq}^-.

Tables S1 to S18 Referred in the Main Text

Table S1. Calculated C−F BDEs (kcal mol^{-1}) for Perfluorocarboxylate Anions (PFCAs).

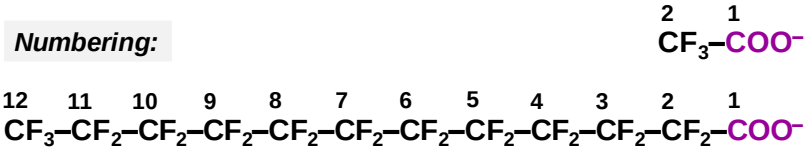

Position	2	3	4	5	6	7	8	9	10	11	12
$CF_3CO_2^-$	116.81										
$C_2F_5CO_2^-$	106.86	119.22									
$C_3F_7CO_2^-$	106.78	110.54	119.20								
$C_4F_9CO_2^-$	106.91	109.03	108.63	118.07							
$C_5F_{11}CO_2^-$	107.22	107.77	107.17	108.42	117.85						
$C_6F_{13}CO_2^-$	107.28	108.37	106.91	106.97	108.36	118.63					
$C_7F_{15}CO_2^-$	107.33	108.06	107.26	107.01	106.78	108.30	117.71				
$C_8F_{17}CO_2^-$	107.34	108.11	107.06	107.14	106.77	106.78	108.32	117.73			
$C_9F_{19}CO_2^-$	107.31	108.03	107.26	107.06	106.87	106.60	106.74	108.32	118.48		
$C_{10}F_{21}CO_2^-$	107.32	108.85	107.25	106.00	106.87	106.79	106.64	106.80	108.06	118.75	
$C_{11}F_{23}CO_2^-$	107.29	107.77	107.25	106.89	106.76	106.74	106.72	106.61	106.80	108.05	117.65

Table S2. Calculated C−F BDEs (kcal mol^{-1}) for Perfluorodicarboxylate Anions (PFdiCAs).

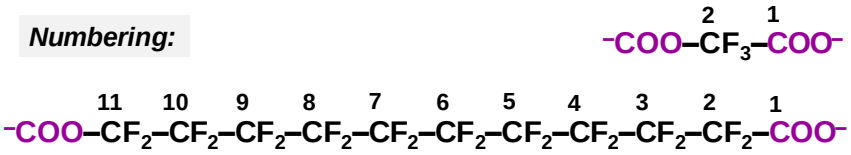

Position	2	3	4	5	6	7	8	9	10	11
$^-O_2CCF_2CO_2^-$	107.27									
$^-O_2CCF_2CH_2CO_2^-$	107.54									
$^-O_2CC_2F_4CO_2^-$	106.66	106.66								
$^-O_2CC_3F_6CO_2^-$	106.94	110.53	106.94							
$^-O_2CC_4F_8CO_2^-$	107.54	109.64	109.64	107.54						
$^-O_2CC_6F_{12}CO_2^-$	107.36	108.38	107.45	107.45	108.38	107.36				
$^-O_2CC_7F_{14}CO_2^-$	107.38	108.31	107.49	107.30	107.49	108.31	107.38			
$^-O_2CC_8F_{16}CO_2^-$	107.32	108.52	107.40	107.25	107.25	107.40	108.52	107.32		
$^-O_2CC_{10}F_{20}CO_2^-$	107.25	107.82	107.31	107.02	106.97	106.97	107.02	107.31	107.82	107.25

Table S3. Calculated C−F BDEs (kcal mol^{-1}) for Fluorotelomer Carboxylate Anions (FTCAs).

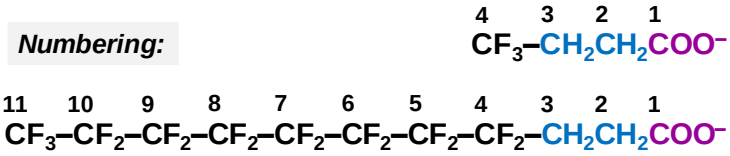

Position	4	5	6	7	8	9	10	11
$CF_3CH_2CH_2CO_2^-$	122.68							
$C_2F_5CH_2CH_2CO_2^-$	113.34	120.59						
$C_3F_7CH_2CH_2CO_2^-$	112.18	110.99	118.82					
$C_4F_9CH_2CH_2CO_2^-$	110.91	109.00	109.43	118.10				
$C_5F_{11}CH_2CH_2CO_2^-$	111.02	110.12	107.02	108.48	118.73			
$C_6F_{13}CH_2CH_2CO_2^-$	110.82	108.97	106.71	106.99	108.37	118.56		
$C_7F_{15}CH_2CH_2CO_2^-$	110.76	108.79	107.19	106.79	106.86	108.17	117.76	
$C_8F_{17}CH_2CH_2CO_2^-$	110.72	108.95	107.11	106.89	106.42	106.78	108.09	118.55

Table S4. Calculated C−F BDEs (kcal mol^{-1}) for Perfluorosulfonate Anions (PFSAs).

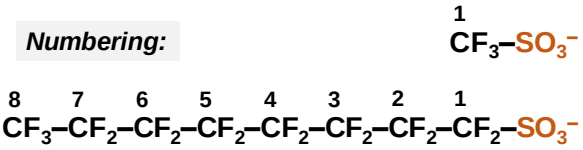

Position	1	2	3	4	5	6	7	8
$CF_3SO_3^-$	119.57							
$C_4F_9SO_3^-$	109.18	106.54	108.85	118.77				
$C_6F_{13}SO_3^-$	109.57	106.38	106.85	106.90	108.41	118.58		
$C_8F_{17}SO_3^-$	112.06	106.73	106.96	106.67	106.67	106.67	108.38	118.80

Table S5. Calculated C−F BDEs (kcal mol^{-1}) for the Three Fluorinated Acetate Anions.

$CF_3CO_2^-$	116.81
$CF_2HCO_2^-$	109.70
$CFH_2CO_2^-$	108.61

Table S6. Peak Areas and Quantification of Transformation Products (TPs) from PFDA Degradation.

(**Note:** only the species (i) with peak areas above the quantification limit and (ii) having standard chemicals are quantified into the molar concentration.)

	PFDA[a]			
Time(h)	**$C_{10}F_{19}O_2^-$**	$C_{10}F_{18}HO_2^-$	$C_{10}F_{17}H_2O_2^-$	$C_{10}F_{16}H_3O_2^-$
0	1.60E+09	1.49E+06	ND	ND
1	1.47E+09	5.08E+07	ND	ND
2	1.11E+09	1.08E+08	3.53E+05	ND
4	6.52E+08	1.90E+08	3.34E+06	ND
8	8.81E+07	1.94E+08	1.11E+07	1.42E+06
12	1.07E+07	1.33E+08	4.70E+06	3.32E+05

	PFNA			**PFOA**	
Time(h)	**$C_9F_{17}O_2^-$**		$C_9F_{16}HO_2^-$	**$C_8F_{15}O_2^-$**	$C_8F_{14}HO_2^-$
0	1.70E+06	<LOQ	ND	1.61E+06	1.11E+05
1	4.81E+07	327 nM	3.48E+05	2.78E+06	9.27E+05
2	5.69E+07	387 nM	1.08E+06	3.51E+06	1.23E+06
4	5.79E+07	394 nM	2.85E+06	3.68E+06	1.72E+06
8	2.32E+07	158 nM	4.48E+06	3.25E+06	8.41E+05
12	1.45E+07	98.4 nM	3.88E+06	3.39E+06	4.45E+05

	PFHpA			**PFHxA**			**PFPeA**		**PFBA**
Time(h)	**$C_7F_{13}O_2^-$**	$C_7F_{12}HO_2^-$	$C_7F_{11}H_2O_2^-$	**$C_6F_{11}O_2^-$**	$C_6F_{10}HO_2^-$	$C_6F_9H_2O_2^-$	**$C_5F_9O_2^-$**	$C_5F_8HO_2^-$	**$C_4F_7O_2^-$**
0	1.90E+05	4.11E+05	ND	7.52E+04	4.28E+05	ND	ND	ND	ND
1	1.95E+06	2.63E+06	ND	8.64E+05	1.80E+06	ND	1.12E+06	4.76E+05	5.36E+05
2	1.85E+06	4.81E+06	2.09E+05	1.70E+06	3.21E+06	7.28E+04	2.15E+06	4.69E+05	7.49E+05
4	1.87E+06	6.77E+06	1.05E+06	2.40E+06	4.22E+06	4.76E+05	3.09E+06	1.20E+06	1.15E+06
8	1.58E+06	2.83E+06	2.97E+06	2.21E+06	1.98E+06	1.45E+06	2.25E+06	6.09E+05	1.11E+06
12	1.47E+06	7.47E+05	3.08E+06	1.72E+06	7.84E+05	1.51E+06	2.15E+06	2.75E+05	7.27E+05

[a]Products with the same chain length are assumed to be H/F exchange derivatives from the corresponding PFCA.

Table S7. Peak Areas and Quantification of TPs from PFNA Degradation.

	PFNA[a]				**PFOA**		
Time(h)	**$C_9F_{17}O_2^-$**	$C_9F_{16}HO_2^-$	$C_9F_{15}H_2O_2^-$	$C_9F_{14}H_3O_2^-$	**$C_8F_{15}O_2^-$**		$C_8F_{14}HO_2^-$
0	1.31E+09	1.59E+07	0.00E+00	0.00E+00	3.76E+06	<LOQ	0.00E+00
1	7.56E+08	8.91E+07	0.00E+00	0.00E+00	4.10E+07	222 nM	0.00E+00
2	3.83E+08	1.36E+08	0.00E+00	0.00E+00	2.79E+07	151 nM	4.50E+05
4	7.97E+07	1.22E+08	3.47E+06	0.00E+00	1.26E+07	<LOQ	1.05E+06
8	2.19E+06	8.07E+07	4.25E+06	3.19E+05	4.09E+06	<LOQ	5.53E+05
12	7.34E+05	6.90E+07	5.52E+06	4.13E+05	3.34E+06	<LOQ	4.44E+05

	PFHpA			**PFHxA**			**PFPeA**		**PFBA**
Time(h)	**$C_7F_{13}O_2^-$**	$C_7F_{12}HO_2^-$	$C_7F_{11}H_2O_2^-$	**$C_6F_{11}O_2^-$**	$C_6F_{10}HO_2^-$	$C_6F_9H_2O_2^-$	**$C_5F_9O_2^-$**	$C_5F_8HO_2^-$	**$C_4F_7O_2^-$**
0	1.02E+07	2.45E+06	0.00E+00	1.01E+06	1.84E+05	0.00E+00	3.97E+05	0.00E+00	0.00E+00
1	5.01E+06	3.16E+06	0.00E+00	8.04E+05	4.44E+06	1.84E+05	1.25E+06	1.67E+06	1.08E+06
2	2.31E+06	2.33E+06	3.98E+05	5.79E+05	4.50E+06	7.60E+05	1.32E+06	1.81E+06	1.34E+06
4	5.44E+05	1.16E+06	1.03E+06	3.19E+05	1.95E+06	1.77E+06	8.44E+05	7.29E+05	9.78E+05
8	3.24E+05	0.00E+00	1.25E+06	2.00E+05	2.07E+05	2.16E+06	4.96E+05	0.00E+00	5.78E+05
12	8.12E+05	0.00E+00	1.24E+06	1.68E+05	1.60E+05	2.00E+06	4.08E+05	0.00E+00	0.00E+00

[a]Products with the same chain length are assumed to be H/F exchange derivatives from the corresponding PFCA.

Table S8. Peak Areas and Quantification of TPs from PFOA Degradation.

	PFOA[a]					
Time(h)	**$C_8F_{15}O_2^-$**	$C_8F_{14}HO_2^-$	$C_8F_{13}H_2O_2^-$	$C_8F_{12}H_3O_2^-$	$C_8F_{11}H_4O_2^-$	$C_8F_9H_6O_2^-$
0	2.84E+09	1.19E+06	6.44E+04	ND	5.17E+05	ND
1	1.74E+09	1.34E+08	5.78E+05	ND	6.53E+05	ND
2	8.99E+08	2.26E+08	2.63E+06	ND	8.66E+05	ND
4	1.61E+08	2.42E+08	8.12E+06	ND	1.37E+06	1.03E+05
8	1.09E+07	1.64E+08	1.31E+07	6.84E+05	1.56E+06	3.90E+05
12	4.79E+06	1.25E+08	1.55E+07	6.85E+05	2.16E+06	5.57E+05
24	4.43E+06	7.79E+07	1.84E+07	8.42E+05	2.69E+06	1.01E+06
36	4.83E+06	6.47E+07	3.40E+07	1.89E+06	4.24E+06	1.07E+06
48	4.91E+06	6.34E+07	3.63E+07	2.12E+06	7.55E+06	8.78E+05

	PFHpA				PFHxA
Time(h)	**$C_7F_{13}O_2^-$**		$C_7F_{12}HO_2^-$	$C_7F_9H_4O_2^-$	$C_6F_{10}HO_2^-$
0	1.27E+07	<LOQ	ND	ND	ND
1	3.74E+07	265 nM	4.57E+05	ND	9.66E+05
2	2.36E+07	167 nM	1.07E+06	ND	8.01E+05
4	7.44E+06	<LOQ	1.15E+06	ND	6.54E+05
8	2.68E+06	<LOQ	8.86E+05	ND	1.58E+05
12	2.25E+06	<LOQ	7.37E+05	1.01E+06	ND
24	1.88E+06	<LOQ	6.33E+05	9.74E+05	ND
36	3.49E+06	<LOQ	8.45E+05	1.93E+06	ND
48	3.66E+06	<LOQ	1.96E+06	2.71E+06	ND

[a]Products with the same chain length are assumed to be H/F exchange derivatives from the corresponding PFCA.

Table S9. Peak Areas and Quantification of TPs from PFHpA Degradation.

	PFHpA[a]			
Time (h)	**$C_7F_{13}O_2^-$**	$C_7F_{12}HO_2^-$	$C_7F_{11}H_2O_2^-$	$C_7F_{10}H_3O_2^-$
0	2.63E+09	3.39E+06	ND	ND
1	1.99E+09	2.13E+08	3.66E+05	ND
2	1.33E+09	3.59E+08	8.87E+05	ND
4	4.52E+08	4.32E+08	3.39E+06	9.87E+04
8	2.14E+07	3.45E+08	8.53E+06	1.96E+05
12	8.79E+05	2.86E+08	4.16E+07	8.76E+05
24	2.05E+05	1.57E+08	3.15E+06	1.84E+05
48	1.43E+05	1.26E+08	4.96E+06	2.61E+05

	PFHxA				PFPeA	
Time (h)	**$C_6F_{11}O_2^-$**		$C_6F_{10}HO_2^-$	$C_6F_9H_2O_2^-$	**$C_5F_9O_2^-$**	$C_5F_8HO_2^-$
0	3.29E+05	<LOQ	1.11E+07	ND	1.57E+05	ND
1	4.29E+07	250 nM	6.95E+06	2.09E+05	2.62E+05	1.72E+05
2	5.44E+07	317 nM	4.04E+06	4.07E+05	3.41E+05	7.90E+05
4	2.09E+07	122 nM	1.45E+06	6.10E+05	6.09E+05	8.40E+05
8	4.70E+06	<LOQ	1.04E+06	4.80E+05	7.66E+05	2.04E+05
12	4.63E+06	<LOQ	8.88E+05	7.34E+05	6.18E+05	ND
24	3.55E+06	<LOQ	5.62E+05	4.05E+05	3.38E+05	ND
48	7.73E+06	<LOQ	8.00E+05	3.08E+05	6.84E+05	ND

[a]Products with the same chain length are assumed to be H/F exchange derivatives from the corresponding PFCA.

Table S10. Peak Areas of TPs from PFHxA Degradation.

	PFHxA[a]			PFPeA	
Time (h)	**$C_6F_{11}O_2^-$**	$C_6F_{10}HO_2^-$	$C_6F_9H_2O_2^-$	**$C_5F_9O_2^-$**	$C_5F_8HO_2^-$
0	2.65E+09	3.27E+07	1.86E+06	3.76E+06	1.06E+05
1	2.01E+09	1.84E+08	2.20E+06	2.97E+07	1.66E+05
2	1.37E+09	3.06E+08	3.67E+06	1.08E+07	2.49E+05
4	4.42E+08	3.62E+08	3.11E+06	8.90E+06	3.59E+05
8	1.78E+07	2.74E+08	1.35E+07	1.27E+06	4.03E+05
12	1.48E+06	2.31E+08	1.68E+07	1.46E+06	3.69E+05

[a]Products with the same chain length are assumed to be H/F exchange derivatives from the corresponding PFCA.

Table S11. Peak Areas of C8 Sulfonate TPs from PFOS Degradation.

	PFOS[a]							
Time(h)	**$C_8F_{17}SO_3^-$**	$C_8F_{16}HSO_3^-$	$C_8F_{15}H_2SO_3^-$	$C_8F_{14}H_3SO_3^-$	$C_8F_{13}H_4SO_3^-$	$C_8F_{12}H_5SO_3^-$	$C_8F_{11}H_6SO_3^-$	$C_8F_9H_8SO_3^-$
0	2.05E+09	ND	ND	ND	ND	ND	ND	ND
1	1.64E+09	2.37E+07	ND	ND	ND	ND	ND	ND
2	1.51E+09	1.99E+07	6.93E+05	9.17E+04	ND	ND	ND	ND
4	1.34E+09	4.05E+07	9.66E+05	1.13E+05	1.17E+05	ND	ND	ND
8	1.09E+09	4.79E+07	1.79E+06	9.36E+05	1.07E+05	ND	5.69E+04	5.56E+04
12	8.29E+08	3.25E+07	1.67E+07	2.50E+06	2.58E+07	ND	ND	1.22E+05
24	5.11E+08	1.87E+07	3.17E+06	2.40E+06	1.28E+06	ND	1.42E+05	2.81E+05
36	3.43E+08	1.73E+07	9.15E+07	6.80E+06	1.02E+07	2.49E+05	ND	2.85E+05
48	2.78E+08	1.36E+07	9.63E+06	3.59E+06	3.68E+06	3.15E+05	1.53E+05	2.70E+05

	PFOS						
Time(h)	$C_8F_8H_9SO_3^-$	$C_8F_7H_{10}SO_3^-$	$C_8F_6H_{11}SO_3^-$	$C_8F_5H_{12}SO_3^-$	$C_8F_4H_{13}SO_3^-$	$C_8F_3H_{14}SO_3^-$	$C_8FH_{16}SO_3^-$
0	ND	ND	ND	ND	ND	ND	ND
1	ND	ND	ND	ND	ND	ND	1.48E+05
2	ND	ND	ND	ND	ND	ND	1.70E+05
4	ND	ND	ND	ND	ND	ND	ND
8	ND	ND	ND	ND	6.77E+04	ND	ND
12	ND	ND	ND	ND	1.27E+05	ND	ND
24	1.43E+05	6.19E+04	8.67E+04	ND	1.38E+05	ND	1.66E+05
36	1.54E+05	5.72E+04	1.63E+05	4.74E+04	1.38E+05	ND	ND
48	1.42E+05	ND	ND	ND	1.13E+05	8.62E+04	ND

[a]Products with the same chain length are assumed to be H/F exchange derivatives from the corresponding PFSA.

Table S12. Peak Areas and Quantification of C7, C6, and C4 Sulfonate TPs from PFOS Degradation.

	PFHpS[a]				
Time(h)	**$C_7F_{15}SO_3^-$**	$C_7F_{14}HSO_3^-$	$C_7F_{13}H_2SO_3^-$	$C_7F_{12}H_3SO_3^-$	$C_7F_{11}H_4SO_3^-$
0	2.84E+08	ND	ND	ND	ND
1	2.37E+08	4.77E+05	ND	ND	ND
2	2.12E+08	9.13E+05	ND	ND	ND
4	1.94E+08	1.34E+06	ND	ND	ND
8	1.53E+08	1.84E+06	1.31E+05	ND	ND
12	1.30E+08	1.65E+06	9.10E+05	ND	ND
24	7.93E+07	1.22E+06	3.10E+05	ND	ND
36	6.71E+07	1.35E+06	5.34E+06	1.33E+05	1.02E+05
48	5.73E+07	1.56E+06	9.16E+05	ND	ND

	PFHxS				**PFBS**		
Time(h)	**$C_6F_{13}SO_3^-$**		$C_6F_{12}HSO_3^-$	$C_6F_{11}H_2SO_3^-$	**$C_4F_9SO_3^-$**	$C_4F_8HSO_3^-$[b]	$C_4F_7H_2SO_3^-$
0	4.50E+07	335 nM	ND	2.72E+05	1.08E+07	1.83E+05	ND
1	1.74E+07	130 nM	2.18E+06	ND	1.05E+07	8.33E+06	ND
2	2.13E+07	158 nM	7.23E+06	ND	1.04E+07	2.12E+07	ND
4	1.63E+07	121 nM	1.45E+07	ND	1.03E+07	4.38E+07	ND
8	1.38E+07	102 nM	2.47E+07	ND	1.01E+07	8.15E+07	ND
12	1.22E+07	<LOQ	3.14E+07	1.59E+05	1.04E+07	1.03E+08	ND
24	9.60E+06	<LOQ	3.76E+07	ND	9.81E+06	1.32E+08	ND
36	8.48E+06	<LOQ	3.23E+07	4.40E+05	9.36E+06	1.37E+08	2.48E+05
48	7.60E+06	<LOQ	3.90E+07	2.50E+05	9.44E+06	1.43E+08	2.25E+05

[a]The C7 PFSA (PFHpS), C6 PFSA (PFHxS) and C4 PFSA (PFBS) in the PFOS reagent have significant peak areas in the t=0 sample, and are thus believed to be impurities from PFOS production. Degradation products with the same chain length are assumed to be H/F exchange derivatives from the corresponding PFSA.

[b]The large peak areas of products with one H/F exchange at 48 h is higher than the perfluorinated sulfonate in the same chain length, probably indicating other mechanisms of formation from longer-chain precursors.

Table S13. Peak Areas of Carboxylate TPs from PFOS Degradation.

	PFOA[a]		**PFHpA**[b]		**PFHxA**[b]		**PFPeA**[b]		**PFBA**[b]
Time(h)	**$C_8F_{15}O_2^-$**	$C_8F_{14}HO_2^-$	**$C_7F_{13}O_2^-$**	$C_7F_{12}HO_2^-$	**$C_6F_{11}O_2^-$**	$C_6F_{10}HO_2^-$	**$C_5F_9O_2^-$**	$C_5F_8HO_2^-$	**$C_4F_7O_2^-$**
0	1.79E+06	ND	7.75E+04	ND	ND	ND	ND	ND	ND
1	1.77E+06	6.92E+04	1.61E+06	ND	5.83E+05	ND	1.60E+06	ND	1.89E+06
2	1.57E+06	1.95E+05	3.28E+06	ND	1.37E+06	ND	3.35E+06	ND	4.03E+06
4	1.23E+06	3.81E+05	3.76E+06	3.81E+05	1.96E+06	1.78E+05	4.17E+06	3.74E+05	5.26E+06
8	6.81E+05	4.77E+05	2.14E+06	8.77E+05	1.30E+06	4.91E+05	2.70E+06	8.50E+05	3.68E+06
12	5.82E+05	5.19E+05	1.56E+06	9.65E+05	1.25E+06	5.47E+05	2.10E+06	9.65E+05	2.70E+06
24	2.73E+05	2.73E+05	6.46E+05	5.33E+05	4.42E+05	4.92E+05	1.24E+06	6.41E+05	1.64E+06
36	1.79E+05	2.16E+05	3.27E+05	3.71E+05	2.24E+05	2.60E+05	8.06E+05	4.75E+05	7.51E+05
48	1.82E+05	2.01E+05	3.82E+05	3.14E+05	3.19E+05	3.12E+05	8.75E+05	4.10E+05	4.82E+05

[a]Products with the same chain length are assumed to be H/F exchange derivatives from the corresponding PFCA.

[b]The ratios of shorter-chain PFCAs to PFOA in this table are much higher than the ratios observed in PFCA degradation reactions (**Table S6-S10**). This indicates that a significant portion of the shorter-chain PFCAs are from the degradation of shorter-chain PFSA impurities in the PFOS reagent (e.g., PFHpS, PFHxS, and PFBS; see Table **S12**).

Table S14. Peak Areas of C6 Sulfonate TPs from PFHxS Degradation.

	PFHxS[a]					
Time(h)	**$C_6F_{13}SO_3^-$**	$C_6F_{12}HSO_3^-$	$C_6F_{11}H_2SO_3^-$	$C_6F_{10}H_3SO_3^-$	$C_6F_9H_4SO_3^-$	$C_6F_6H_7SO_3^-$
0	4.45E+09	ND	ND	ND	ND	ND
1	3.29E+09	5.84E+06	ND	ND	ND	ND
2	3.22E+09	1.25E+07	1.38E+06	ND	1.00E+05	ND
4	3.31E+09	2.43E+07	3.24E+06	ND	1.53E+05	ND
8	2.93E+09	4.36E+07	3.05E+07	8.48E+04	1.65E+05	3.85E+05
12	2.97E+09	4.90E+07	5.20E+07	3.43E+05	1.54E+05	3.99E+05
24	2.69E+09	5.82E+07	8.90E+07	8.30E+05	1.83E+05	4.48E+05
36	2.75E+09	6.10E+07	1.22E+08	1.19E+06	2.39E+05	4.24E+05
48	2.72E+09	5.74E+07	8.50E+07	1.19E+06	ND	5.85E+05

[a]Products with the same chain length are assumed to be H/F exchange derivatives from the corresponding PFSA.

Table S15. Peak Areas of C5, C4, and C3 Sulfonate TPs from PFHxS Degradation.

	PFPeS[a]		PFBS		PFPrS
Time(h)	**$C_5F_{11}SO_3^-$**	$C_5F_{10}HSO_3^-$	**$C_4F_9SO_3^-$**	$C_4F_8HSO_3^-$[b]	$C_3F_6HSO_3^-$
0	2.20E+07	ND	1.18E+07	0.00E+00	0.00E+00
1	2.09E+07	ND	1.12E+07	1.47E+06	7.72E+05
2	2.03E+07	ND	1.10E+07	3.28E+06	2.72E+06
4	2.13E+07	ND	1.20E+07	1.50E+07	4.08E+06
8	1.90E+07	2.05E+05	1.13E+07	1.44E+07	9.08E+06
12	1.99E+07	4.12E+05	1.19E+07	2.13E+07	2.42E+07
24	1.64E+07	5.01E+05	1.09E+07	2.99E+07	2.07E+07
36	1.85E+07	6.09E+05	1.17E+07	3.51E+07	4.12E+07
48	1.72E+07	6.71E+05	1.14E+07	4.83E+07	2.37E+07

[a]Products with the same chain length are assumed to be H/F exchange derivatives from the corresponding PFSA.

[b]The peak areas of products with one H/F exchange at 48 h are higher than the perfluorinated sulfonate in the same chain length, probably indicating other mechanisms of formation from longer-chain precursors.

Table S16. Peak Areas of Carboxylate TPs from PFHxS Degradation.

	PFHxA[a]			PFPeA[b]		PFBA[b]
Time(h)	**$C_6F_{11}O_2^-$**	$C_6F_{10}HO_2^-$	$C_6F_9H_2O_2^-$	**$C_5F_9O_2^-$**	$C_5F_8HO_2^-$	**$C_4F_7O_2^-$**
0	1.32E+05	3.63E+05	ND	ND	ND	ND
1	2.04E+06	1.83E+05	ND	2.16E+06	ND	ND
2	2.68E+06	3.98E+05	ND	4.24E+06	ND	3.54E+05
4	3.09E+06	1.01E+06	ND	5.51E+06	3.07E+05	5.65E+05
8	2.26E+06	1.67E+06	7.49E+04	3.58E+06	6.88E+05	5.95E+05
12	2.00E+06	2.05E+06	1.12E+05	3.24E+06	9.48E+05	8.58E+05
24	1.84E+06	2.17E+06	2.31E+05	2.55E+06	9.50E+05	3.64E+05
36	2.01E+06	2.58E+06	3.30E+05	2.43E+06	9.58E+05	3.15E+05
48	2.23E+06	2.32E+06	2.75E+05	2.97E+06	9.38E+05	3.51E+05

[a]Products with the same chain length are assumed to be H/F exchange derivatives from the corresponding PFCA.

[b]The ratios of shorter-chain PFCAs to PFOA in this table are much higher than the ratios observed in PFCA degradation reactions (**Table S6**-**S10**). This indicates that a significant portion of the shorter-chain PFCAs are from the degradation of shorter-chain PFSA impurities in the PFHxS reagent (e.g., PFPeS and PFBS; see Table **S15**).

Table S17. Peak Areas and Quantification of Telomeric Carboxylate TPs from n=8 FTCA Degradation.

	n=8 FTCA ($C_8F_{17}CH_2CH_2COO^-$)[a]			**n=6 FTCA[b]**			**n=5 FTCA[b]**		**n=4 FTCA**
Time(h)	**$C_{11}F_{17}H_4O_2^-$**	$C_{11}F_{16}H_5O_2^-$	$C_{11}F_{15}H_6O_2^-$	**$C_9F_{13}H_4O_2^-$**		$C_9F_{12}H_5O_2^-$	**$C_8F_{11}H_4O_2^-$**	$C_8F_{10}H_5O_2^-$	$C_7F_8H_5O_2^-$
0	7.99E+08	ND	ND	ND	<LOQ	ND	ND	ND	ND
1	7.91E+08	1.93E+06	ND	ND	<LOQ	9.51E+04	ND	5.85E+05	2.73E+05
2	7.37E+08	4.22E+06	1.54E+05	1.04E+05	<LOQ	2.48E+05	ND	1.32E+06	6.19E+05
4	7.92E+08	7.93E+06	7.71E+05	1.96E+05	<LOQ	9.04E+05	8.84E+04	3.26E+06	1.50E+06
8	6.42E+08	5.46E+06	1.32E+06	4.28E+05	10.5 nM	2.27E+06	1.55E+05	6.43E+06	3.01E+06
12	5.75E+08	5.42E+06	2.86E+06	5.94E+05	14.6 nM	2.97E+06	2.23E+05	9.08E+06	4.37E+06
24	4.40E+08	3.71E+06	2.92E+06	7.68E+05	18.9 nM	4.58E+06	3.67E+05	1.31E+07	6.65E+06
36	2.61E+08	4.46E+06	1.37E+07	8.96E+05	22.0 nM	3.17E+06	3.74E+05	1.54E+07	7.47E+06
48	2.42E+08	4.03E+06	1.03E+07	9.31E+05	22.9 nM	4.63E+06	4.09E+05	1.63E+07	8.49E+06

[a]Products with the same chain length and containing more than 5 hydrogens are assumed to be H/F exchange derivatives from the corresponding FTCA. Note that perfluorinated carboxylates did not yield detectable products with more than 4 H/F exchanges.

[b]Unlike shorter-chain PFSAs in PFOS and PFHxS degradation samples, these shorter-chain FTCAs are not impurities in the n=8 FTCA reagent because they were not detected in the t=0 sample.

Table S18. Peak Areas and Quantification of Carboxylate TPs from n=8 FTCA Degradation.

	PFOA[a]	**PFHpA**	**PFHxA**	**PFPeA**	**PFBA**
Time(h)	**$C_8F_{15}O_2^-$**	**$C_7F_{13}O_2^-$**	**$C_6F_{11}O_2^-$**	**$C_5F_9O_2^-$**	**$C_4F_7O_2^-$**
0	1.71E+05	ND	ND	ND	ND
1	ND	ND	ND	ND	6.60E+05
2	1.54E+05	ND	ND	ND	1.40E+06
4	1.84E+05	ND	ND	1.24E+05	2.23E+06
8	1.98E+05	ND	ND	1.30E+05	1.96E+06
12	2.17E+05	ND	ND	9.90E+04	1.58E+06
24	2.31E+05	6.09E+04	ND	1.05E+05	9.88E+05
36	4.23E+05	1.05E+05	7.68E+04	8.23E+04	7.17E+05
48	5.54E+05	1.84E+05	1.78E+05	1.48E+05	6.54E+05

[a]Products with H/F exchanges from perfluorinated carboxylates were not detected.

Figures S1 to S4 Referred in the Main Text

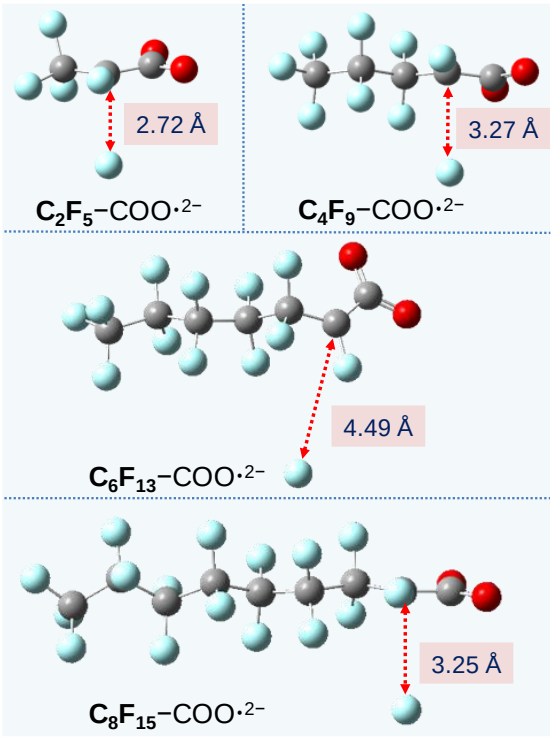

Figure S1. Geometry-optimized structure of n=2, 4, 6, and 8 PFCA·$^{2-}$ at the B3LYP-D3(BJ)/6-311+G(2d,2p) level of theory.

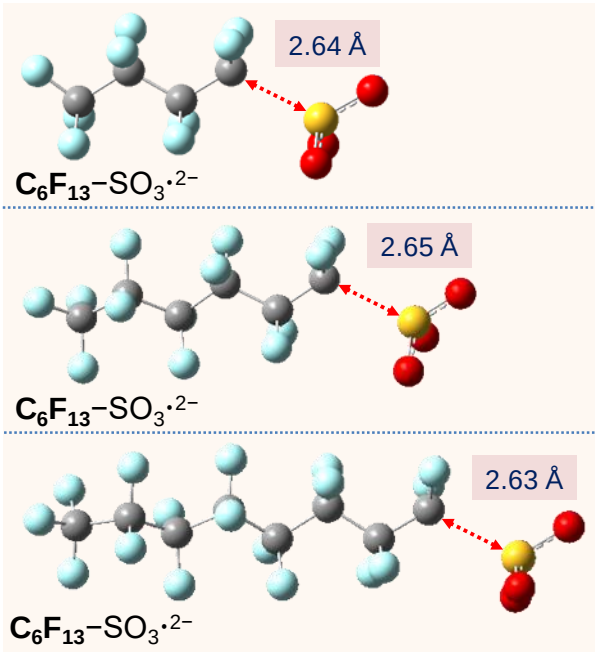

Figure S2. Geometry-optimized structure of n=4, 6, and 8 PFSA·$^{2-}$ at the B3LYP-D3(BJ)/6-311+G(2d,2p) level of theory.

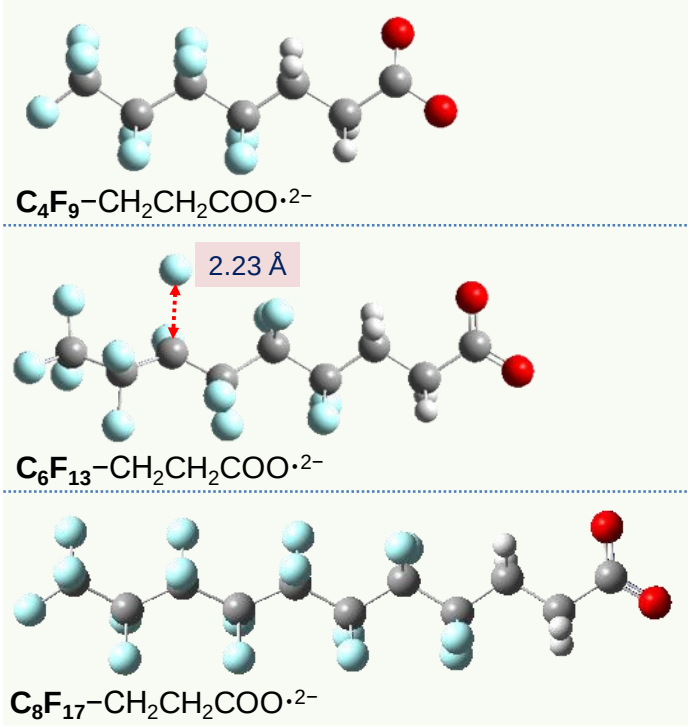

Figure S3. Geometry-optimized structure of n=4, 6, and 8 $FTCA^{\cdot 2-}$ at the B3LYP-D3(BJ)/6-311+G(2d,2p) level of theory.

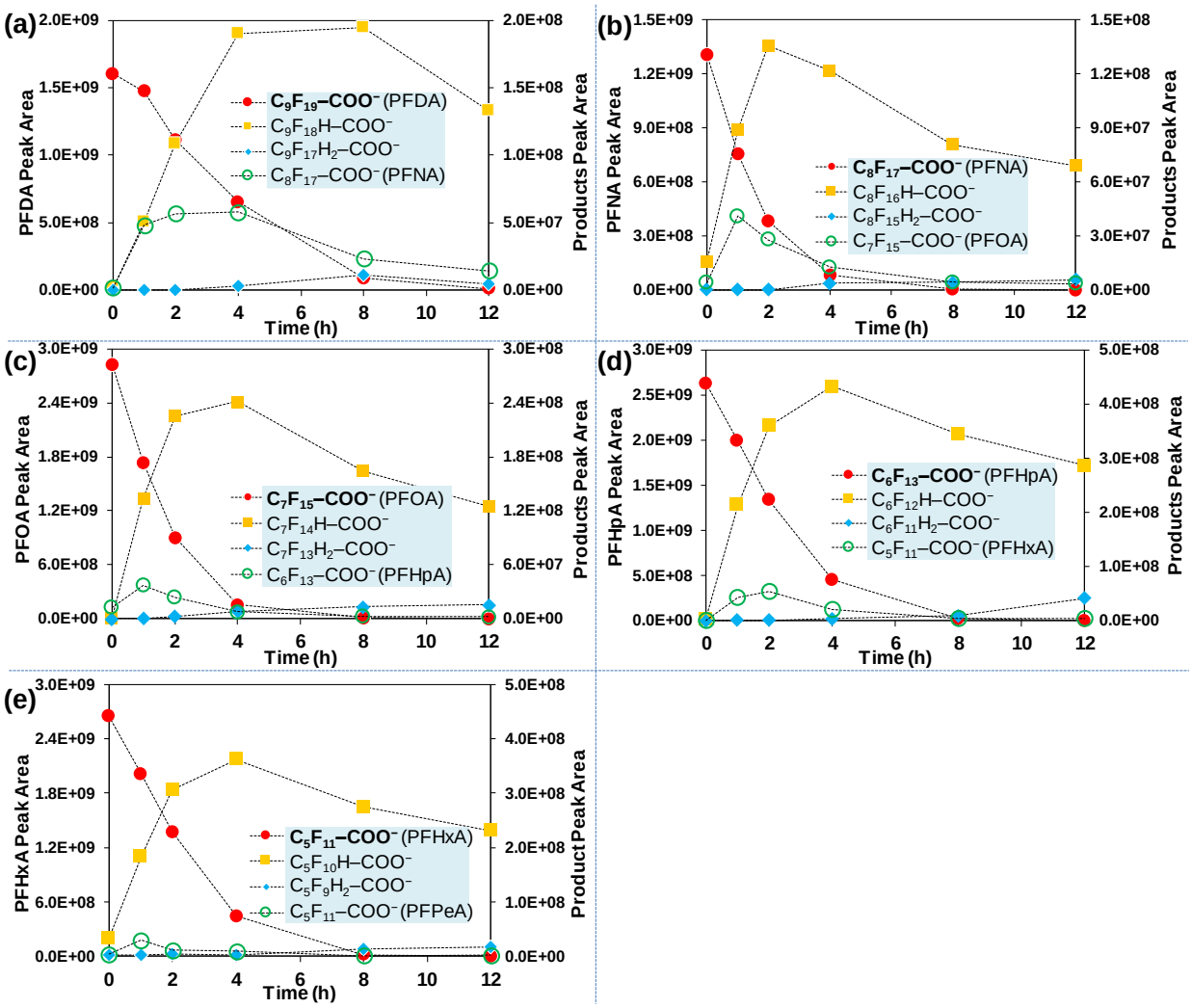

Figure S4. Representative degradation products from **(a)** PFDA, **(b)** PFNA, **(c)** PFOA, **(d)** PFHpA, and **(e)** PFHxA. All detected species including those in low intensities are summarized in **Tables S6**–**S18**.

Text S1 Referred in the Main Text

Text S1. In general, the C−F BDE for −CH*F*− is lower than that of –CF_2–, whereas the C−F BDE for –CF_2−CH_2– is higher than that of –CF_2−CF_2–.

For the former case, the increasing number of F atoms on the same (geminal) C atom will increase the positive partial charge on the C atom. This would increase the ionic character of the C−F bond, leading to an elevated BDE.[19] This theory is supported by comparing C−F BDEs among CF_4, CF_3H, CF_2H_2, and CFH_3,[19] and between CF_3CF_3 and CH_3CH_2F.[20]

For the latter case, the fluorocarbon group −CF_2– or –CF_3 is a strong electron-withdrawing group to weaken the C−F bonds on the neighboring –CF_2− group. The hydrocarbon group does not have such an effect to weaken the C−F bonds on the neighboring –CF_2− group. This theory is supported by the calculated C−F BDEs of PFCAs and FTCAs in this study. More examples can be found from Liu *et al.*[17] where a variety of branched PFASs structures were calculated.

We examined two polyfluorinated alcohols (**Figure S5**) as the probe compounds. The structure **(structure b)** with −CH*F*− in the middle of the fluorocarbon chain indeed showed (i) lower C−F BDE and (ii) much faster defluorination in comparison to the one with –CF_2− in the middle of the fluorocarbon chain **(structure a)**.

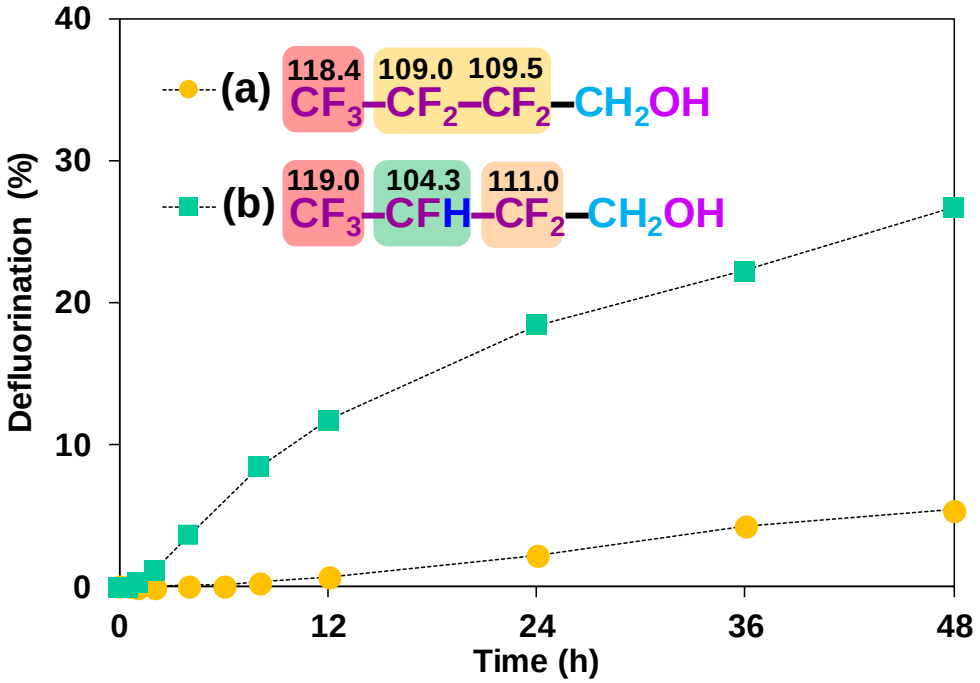

Figure S5. Time profiles for the defluorination of two probing fluorinated alcohols. Reaction conditions: PFAS (0.025 mM), Na_2SO_3 (10 mM), carbonate buffer (5 mM), 254 nm irradiation (18 W low-pressure Hg lamp), pH 9.5 and 20 °C. Numbers on the top of each molecule show the calculated C–F BDEs (kcal mol^{-1}) at the B3LYP-D3(BJ)/6-311+G(2d,2p) level of theory.

References

1. Li, X.; Ma, J.; Liu, G.; Fang, J.; Yue, S.; Guan, Y.; Chen, L.; Liu, X., Efficient reductive dechlorination of monochloroacetic acid by sulfite/UV process. *Environ. Sci. Technol.* **2012,** *46*, (13), 7342-7349.

2. Srivastava, R. K.; Jozewicz, W., Flue gas desulfurization: the state of the art. *J. Air Waste Manag. Assoc.* **2001,** *51*, (12), 1676-1688.

3. Gu, Y.; Dong, W.; Luo, C.; Liu, T., Efficient reductive decomposition of perfluorooctanesulfonate in a high photon flux UV/sulfite system. *Environ. Sci. Technol.* **2016,** *50*, (19), 10554-10561.

4. Gu, Y.; Liu, T.; Zhang, Q.; Dong, W., Efficient decomposition of perfluorooctanoic acid by a high photon flux UV/sulfite process: Kinetics and associated toxicity. *Chem. Eng. J.* **2017,** *326*, 1125-1133.

5. Qu, Y.; Zhang, C.; Li, F.; Chen, J.; Zhou, Q., Photo-reductive defluorination of perfluorooctanoic acid in water. *Water Res.* **2010,** *44*, (9), 2939-2947.

6. Song, Z.; Tang, H.; Wang, N.; Zhu, L., Reductive defluorination of perfluorooctanoic acid by hydrated electrons in a sulfite-mediated UV photochemical system. *J. Hazard. Mater.* **2013,** *262*, 332-338.

7. Sun, Z.; Zhang, C.; Xing, L.; Zhou, Q.; Dong, W.; Hoffmann, M. R., UV/Nitrilotriacetic Acid Process as a Novel Strategy for Efficient Photoreductive Degradation of Perfluorooctanesulfonate. *Environ. Sci. Technol.* **2018,** *52*, (5), 2953-2962.

8. Park, H.; Vecitis, C. D.; Cheng, J.; Choi, W.; Mader, B. T.; Hoffmann, M. R., Reductive defluorination of aqueous perfluorinated alkyl surfactants: effects of ionic headgroup and chain length. *J. Phys. Chem. A* **2009,** *113*, (4), 690-696.

9. Yu, Y.; Han, P.; Zhou, L.-J.; Li, Z.; Wagner, M.; Men, Y., Ammonia monooxygenase-mediated cometabolic biotransformation and hydroxylamine-mediated abiotic transformation of micropollutants in an AOB/NOB coculture. *Environ. Sci. Technol.* **2018,** *52*, (16), 9196-9205.

10. Men, Y.; Han, P.; Helbling, D. E.; Jehmlich, N.; Herbold, C.; Gulde, R.; Onnis-Hayden, A.; Gu, A. Z.; Johnson, D. R.; Wagner, M.; Fenner, K., Biotransformation of two pharmaceuticals by the ammonia-oxidizing archaeon *Nitrososphaera gargensis*. *Environ. Sci. Technol.* **2016,** *50*, (9), 4682-4692.

11. Frisch, M. J.; Trucks, G. W.; Schlegel, H. B.; Scuseria, G. E.; Robb, M. A.; Cheeseman, J. R.; Scalmani, G.; Barone, V.; Petersson, G. A.; Nakatsuji, H.; Li, X.; Caricato, M.; Marenich, A. V.; Bloino, J.; Janesko, B. G.; Gomperts, R.; Mennucci, B.; Hratchian, H. P.; Ortiz, J. V.; Izmaylov, A. F.; Sonnenberg, J. L.; Williams; Ding, F.; Lipparini, F.; Egidi, F.; Goings, J.; Peng, B.; Petrone, A.; Henderson, T.; Ranasinghe, D.; Zakrzewski, V. G.; Gao, J.; Rega, N.; Zheng, G.; Liang, W.; Hada, M.; Ehara, M.; Toyota, K.; Fukuda, R.; Hasegawa, J.; Ishida, M.; Nakajima, T.; Honda, Y.; Kitao, O.; Nakai, H.; Vreven, T.; Throssell, K.; Montgomery Jr., J. A.; Peralta, J. E.; Ogliaro, F.; Bearpark, M. J.; Heyd, J. J.; Brothers, E. N.; Kudin, K. N.; Staroverov, V. N.; Keith, T. A.; Kobayashi, R.; Normand, J.; Raghavachari, K.; Rendell, A. P.; Burant, J. C.; Iyengar, S. S.; Tomasi, J.; Cossi, M.; Millam, J. M.; Klene, M.; Adamo, C.; Cammi, R.; Ochterski, J. W.; Martin,

R. L.; Morokuma, K.; Farkas, O.; Foresman, J. B.; Fox, D. J. *Gaussian 16 Rev. B.01*, Wallingford, CT, 2016.

12. Grimme, S.; Ehrlich, S.; Goerigk, L., Effect of the damping function in dispersion corrected density functional theory. *J. Comput. Chem.* **2011,** *32*, (7), 1456-1465.

13. Becke, A. D., Density-functional thermochemistry. III. The role of exact exchange. *J. Chem. Phys.* **1993,** *98*, (7), 5648-5652.

14. Lee, C.; Yang, W.; Parr, R. G., Development of the Colle-Salvetti correlation-energy formula into a functional of the electron density. *Phys. Rev. B* **1988,** *37*, (2), 785.

15. Stephens, P.; Devlin, F.; Chabalowski, C.; Frisch, M. J., Ab initio calculation of vibrational absorption and circular dichroism spectra using density functional force fields. *J. Phys. Chem.* **1994,** *98*, (45), 11623-11627.

16. Vosko, S. H.; Wilk, L.; Nusair, M., Accurate spin-dependent electron liquid correlation energies for local spin density calculations: a critical analysis. *Can. J. Phys.* **1980,** *58*, (8), 1200-1211.

17. Liu, J.; Van Hoomissen, D. J.; Liu, T.; Maizel, A.; Huo, X.; Fernández, S. R.; Ren, C.; Xiao, X.; Fang, Y.; Schaefer, C. E., Reductive defluorination of branched per-and polyfluoroalkyl substances with cobalt complex catalysts. *Environ. Sci. Technol. Lett.* **2018,** *5*, (5), 289-294.

18. Marenich, A. V.; Cramer, C. J.; Truhlar, D. G., Universal solvation model based on solute electron density and on a continuum model of the solvent defined by the bulk dielectric constant and atomic surface tensions. *J. Phys. Chem. B* **2009,** *113*, (18), 6378-6396.

19. Lemal, D. M., Perspective on fluorocarbon chemistry. *J. Org. Chem.* **2004,** *69*, (1), 1-11.

20. Krafft, M. P.; Riess, J. G., Selected physicochemical aspects of poly-and perfluoroalkylated substances relevant to performance, environment and sustainability—Part one. *Chemosphere* **2015,** *129*, 4-19.